The Plant Cell, Vol. 19: 904–913, March 2007, www.plantcell.org © 2007 American Society of Plant Biologists

A Core Subunit of the RNA-Processing/Degrading Exosome Specifically Influences Cuticular Wax Biosynthesis in *Arabidopsis* [W]

Tanya S. Hooker,[1] Patricia Lam, Huanquan Zheng,[2] and Ljerka Kunst[3]

Department of Botany, University of British Columbia, Vancouver, British Columbia, V6T 1Z4, Canada

The cuticle is an extracellular matrix composed of cutin polyester and waxes that covers aerial organs of land plants and protects them from environmental stresses. The *Arabidopsis thaliana cer7* mutant exhibits reduced cuticular wax accumulation and contains considerably lower transcript levels of *ECERIFERUM3*/*WAX2*/*YORE-YORE* (*CER3*/*WAX2*/*YRE*), a key wax biosynthetic gene. We show here that CER7 protein is a putative 3′-5′ exoribonuclease homologous to yeast Ribonuclease PH45 (RRP45p), a core subunit of the RNA processing and degrading exosome that controls the expression of *CER3*/*WAX2*/*YRE*. We propose that CER7 acts by degrading a specific mRNA species encoding a negative regulator of *CER3*/*WAX2*/*YRE* transcription. A second RRP45p homolog found in *Arabidopsis*, designated At RRP45a, is partially functionally redundant with CER7, and complete loss of RRP45 function in *Arabidopsis* is lethal. To our knowledge, CER7 is currently the only example of a core exosomal subunit specifically influencing a cellular process.

INTRODUCTION

The epidermal cells of primary organs of all land plants are covered with a cuticle, a continuous lipid layer that limits nonstomatal water loss, prevents organ fusion during development (Lolle et al., 1998; Sieber et al., 2000), and protects plants against numerous biotic and abiotic environmental factors, including bacterial and fungal pathogens, temperature extremes, and UV light. The cuticle is composed of cutin, an insoluble polyester of C16 and C18 hydroxy and epoxy fatty acids and glycerol (Graça et al., 2002; Nawrath, 2002) that is surrounded and covered with waxes, predominantly aliphatic derivatives of very long chain fatty acids easily extracted with organic solvents (Kunst and Samuels, 2003).

In recent years, genetic studies have yielded some insights into wax biosynthetic pathways (Kunst et al., 2006) and uncovered a transporter that can move wax constituents across the plasma membrane (Pighin et al., 2004). However, little is known about the regulation of cuticular wax deposition, an issue of fundamental importance for the development of plant cultivars with improved cuticle properties that are more resistant to environmental stresses. Currently, the only regulatory proteins known to affect wax production are the WAX INDUCER1/SHINE family in *Arabidopsis thaliana* and WAX PRODUCTION ACTIVATOR1 in *Medicago truncatula* (Aharoni et al., 2004; Broun et al., 2004; Zhang et al., 2005). Overexpression of these APETALA2/ETHYLENE RESPONSE FACTOR–type transcription factors dramatically enhances wax accumulation in leaves of transgenic plants, but their in planta roles in regulating wax deposition have not yet been confirmed by analysis of loss-of-function mutants.

To identify mutants defective in regulation of wax production, we examined the expression of the cloned wax biosynthetic genes in all the wax-deficient *eceriferum* (*cer*) lines of *Arabidopsis* described by Koornneef et al. (1989). The *cer7* mutant was found to have reduced transcript levels of *CER3*/*WAX2*/*YORE-YORE* (*YRE*) (*CER3* is allelic to *WAX2*/*YRE*; O. Rowland and L. Kunst, unpublished data), a gene that encodes a protein of unknown function required for the production of ~80% of wax in *Arabidopsis* stems (Chen et al., 2003; Kurata et al., 2003). We therefore hypothesized that the CER7 protein was a regulator of wax biosynthesis that acts by controlling the levels of *CER3*/*WAX2*/*YRE* transcription. To examine if this is indeed the case, we identified the *CER7* gene by a map-based approach and investigated the mechanism by which the CER7 protein controls cuticular wax deposition.

RESULTS

The *cer7* Mutant Phenotype and Cloning of the *CER7* Gene

The recessive *cer7-1* mutant allele with bright green glossy stems and siliques in the Landsberg *erecta* (L*er*) background of *Arabidopsis* was first described by Koornneef et al. (1989). Cuticular wax analysis of *cer7* plants indicated that the stem and silique wax loads were reduced to ~30% (Goodwin et al., 2005; Figure 1) and 50% of wild-type levels, respectively, whereas the leaf wax load was similar to that of the wild type (Figure 1). A positional cloning approach was used to identify the *CER7* gene, which had been previously mapped to 87.1 centimorgans

[1] Current address: School of Biological Sciences, University of Missouri-Kansas City, Kansas City, MO 64110.
[2] Current address: Department of Biology, McGill University, Montreal, Quebec, H3A 1B1, Canada.
[3] To whom correspondence should be addressed. E-mail kunst@interchange.ubc.ca; fax 604-822-6089.
The author responsible for distribution of materials integral to the findings presented in this article in accordance with the policy described in the Instructions for Authors (www.plantcell.org) is: Ljerka Kunst (kunst@interchange.ubc.ca).
[W] Online version contains Web-only data.
www.plantcell.org/cgi/doi/10.1105/tpc.106.049304

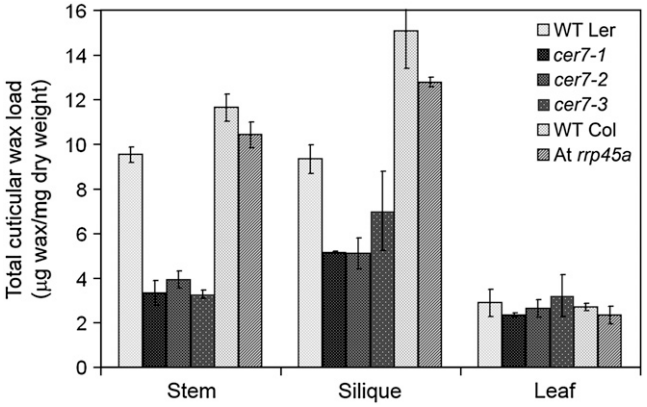

Figure 1. *cer7* Mutants Have Reduced Cuticular Wax Loads on Stems and Siliques.

Total wax loads on stems, siliques, and leaves of wild-type, *cer7*, and At *rrp45a* plants. Each bar represents the mean of three independent analyses of wax extracts from three pooled individuals ± SD.

on chromosome 3 (Koornneef et al., 1989) (Figure 2A). Complementation with a genomic fragment including the *At3g60500* coding sequence and 1.4 and 0.3 kb of 5′ and 3′ sequence, respectively, rescued the wax deficiency of the *cer7-1* mutant, demonstrating that it is the *CER7* gene (Figure 2B). We identified two additional alleles of *CER7* in the T-DNA insertional mutant collections: *cer7-2* (SALK_003100; Alonso et al., 2003) and *cer7-3* (SAIL_747_B08; Sessions et al., 2002). Neither of these mutants was able to complement *cer7-1* in crosses. Sequencing of *At3g60500* in the *cer7-1* mutant identified a point mutation, a substitution of C to T at nucleotide 532 of the open reading frame. This mutation introduces a premature stop codon that would severely truncate the protein and likely inactivate it (Figure 2C). The T-DNA insertion in the *cer7-2* allele was located in the 5′ promoter region, while *cer7-3* was disrupted in the 7th exon of *CER7* (Figure 2C). RT-PCR amplification of the *CER7* coding sequence using RNA isolated from stems showed that the abundance of *CER7* transcript was similar to the wild type in *cer7-1*, that *cer7-2* has reduced levels of *CER7* transcript, and that the *cer7-3* allele has no detectable full-length transcript (Figure 2D). In addition to the wax deficiency observed in all three *cer7* alleles, *cer7-3* mutant seeds had low viability. When every seed from nine siliques was sown on an agar plate, only 14 of the 387 seeds germinated. Transformation of the *cer7-3* mutant with the *At3g60500* genomic fragment complemented both the wax deficiency and the seed viability phenotype (Figure 6B; data not shown).

CER7 Encodes an Exosomal Exoribonuclease-Like Protein

Analysis of the predicted 439–amino acid CER7 protein revealed that it has a conserved RNase PH domain and exhibits 42% identity with a human POLYMYOSITIS/SCLERODERMA75 (PM/Scl-75) protein and 38% identity with the yeast RRP45p (Figure 3). The yeast and human homologs have been characterized as 3′-5′ exoribonucleases, core subunits of the RNA-processing and degrading exosome (Butler, 2002; Raijmakers et al., 2004). The yeast and human exosomes contain six RNase PH subunits arranged in a ring-like structure similar to the bacterial POLYNUCLEOTIDE PHOSPHORYLASE enzyme (Liu et al., 2007). An *Arabidopsis* homolog for one of these subunits, yeast RRP41p, has been characterized (Chekanova et al., 2000). In the *Arabidopsis* genome, there are seven annotated open reading frames with homology to the RNase PH family of exosomal proteins. A bootstrapped neighbor-joining tree of the *Arabidopsis*, yeast (*Saccharomyces cerevisiae*), and human RNase PH protein sequences (Figure 4) shows that CER7 groups with the human and yeast RRP45 homologs, with 99% bootstrap support. An additional member of this clade is the *At3g12990* gene product from *Arabidopsis*, designated At RRP45a. CER7 and At RRP45a are 88% identical over amino acids 1 to 307 (Figure 3). However, the CER7 protein is 132 amino acids longer than At RRP45a and has a putative nuclear localization signal (absent from At RRP45a) at its C terminus, suggesting that the subcellular localization or the mechanism of nuclear import of these two proteins may be different.

CER7 and At RRP45a Functions Partially Overlap

To determine whether there is a specific function associated with At RRP45a that diverges from that of CER7, we obtained two lines, SALK_064229 and GABI_655D02 (Li et al., 2003; Rosso et al., 2003), with T-DNA insertion points just before the 5′ untranslated region and in the 6th exon, respectively. Expression analysis by RT-PCR showed that the abundance of At *RRP45a* transcript was similar to the wild type in SALK_064229 but that the GABI_655D02 line designated At *rrp45a* (Figures 2C and 2D) had no detectable full-length transcript. However, the At *rrp45a* mutant had no visible phenotype, even though wax analysis data indicate a minor reduction in silique, stem, and leaf wax content.

To establish the extent of the functional overlap between the two apparent *Arabidopsis* homologs, CER7 and At RRP45a, we examined their expression domains, subcellular distribution, and their ability to complement the yeast *rrp45* and the *Arabidopsis* *cer7-3* mutants. Expression analyses showed that both *CER7* and At *RRP45a* were transcribed in all tissues, including the stem epidermis involved in cuticular wax synthesis (Figures 5A and 5B). To visualize CER7 and At RRP45a in planta, green fluorescent protein (GFP) fusions of both proteins were transiently expressed in tobacco (*Nicotiana tabacum*) under the constitutive 35S promoter. Examination of tobacco epidermal cells revealed that CER7:GFP and At RRP45a:GFP were both localized in the cytoplasm and the nucleus but specifically excluded from the nucleolus (Figure 5C). Since this pattern is very similar to that seen for GFP alone, we confirmed that the transformed cells were expressing full-length fusion proteins by a protein gel blot (data not shown). We also observed an identical localization pattern, but with a weaker GFP signal, using stably transformed *cer7-1* plants whose waxless phenotype was complemented by the CER7:GFP protein (data not shown).

To test whether CER7 and At RRP45a proteins can both perform exosomal functions in yeast cells, the plant cDNA clones were introduced into a yeast *rrp45* null mutant (Allmang et al., 1999a) under the control of the constitutive GDP promoter. The introduction of the *CER7* cDNA complemented the yeast mutant phenotype (Figure 6A), allowing growth and the formation of

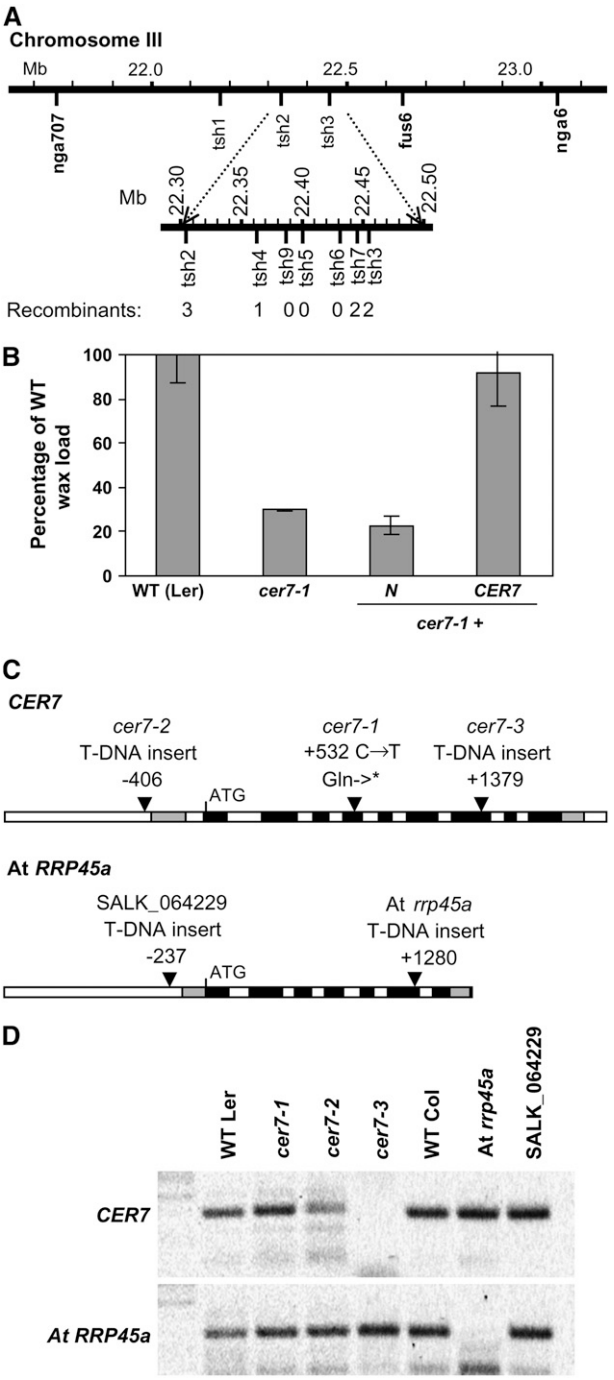

Figure 2. *CER7* and At *RRP45a* Gene Structures and Transcript Levels in *cer7* and At *rrp45a* Mutants.

(A) Schematic representation of the chromosomal location of *CER7* and markers used to fine-map the locus.

(B) Stem wax loads relative to the wild type (*Ler*) of *cer7-1* and *cer7-1* transformed with a noncomplementing gene (*cer7-1* + *N*) and *At3g60500* (*cer7-1* + *CER7*). Bars represent means ± SD ($n = 3, 3, 3,$ and 10).

(C) Schematic representation of the *CER7* (*At3g60500*) and At *RRP45a* (*At3g12990*) gene structures, including the coding sequences (exons, black; introns, white), 5′ and 3′ untranslated regions (gray), and upstream and downstream sequences (white). The positions and types of lesions of the *cer7* and At *rrp45a* mutant alleles are indicated.

(D) RT-PCR analysis of *CER7* and At *RRP45a* transcript levels in *cer7* and At *rrp45a* mutants compared with the corresponding wild types.

colonies. Introduction of the At *RRP45a* cDNA also partially rescued the *rrp45* yeast mutant but was much less effective than *CER7*. In addition, we expressed the *cer7-1* cDNA in yeast and found that it was unable to complement the mutant phenotype, confirming that the *cer7-1* mutant protein is inactive.

To investigate if the C-terminal domain unique to CER7 is relevant to its function in cuticular wax deposition, we introduced a stop codon into the *CER7* genomic clone to correspond to the stop codon encoded in the At *RRP45a* gene and attempted to complement the *cer7-3* mutant with this truncated *CER7* variant. Wax loads from 20 independent transgenic lines carrying the truncated *CER7* gene were only slightly lower than those of *cer7-3* plants transformed with the *CER7* genomic clone (Figure 6B), indicating that the 132–amino acid C-terminal extension of CER7 is not essential for its wax regulatory function.

To extend our functional assessment of CER7 and At RRP45a proteins, we compared their ability to complement the *cer7* mutant. Expression of either gene in the *cer7-3* mutant background using the *CER7* promoter rescued the *cer7* wax deficiency (Figure 6B). Collectively, these data indicate that CER7 and At RRP45a proteins have mostly redundant functions and that they can both mediate wax deposition in *Arabidopsis*.

Loss-of-function mutations in core exosome subunits, including RRP45, are virtually lethal in yeast, with *rrp45* mutants capable of only very limited growth (Allmang et al., 1999a). Given the poor seed viability of the *cer7-3* allele even in the presence of wild-type At *RRP45a*, we expected that the disruption of both of these genes would result in embryo lethality. To test this hypothesis, we crossed the At *rrp45a* mutant with *cer7-3*. Of 1078 F2 progeny from this cross, 131 plants exhibited the *cer7* wax-deficient phenotype. Genotyping of these *cer7* plants showed that none of them was homozygous for a mutation at the At *RRP45a* locus, suggesting that the double mutant is not viable.

Furthermore, an examination of the developing seeds in five siliques from each of four individual F2 progeny that were homozygous for the At *rrp45a* mutant allele and heterozygous for the *cer7-3* allele revealed that only 51.4% of the seeds matured. This ratio suggests that the double mutation is gametophytic lethal. Alexander staining of the pollen from these F2 plants showed that a large percentage of the pollen was also inviable.

To further verify the transmission of the *cer7-3* mutant allele in the At *rrp45a* mutant background, several of these F2 progeny were test-crossed to the At *rrp45a* mutant. None of the 13 progeny obtained when the At *rrp45a* homozygote/*cer7-3* heterozygote was used as the female parent or the 40 progeny obtained when the At *rrp45a* homozygote/*cer7-3* heterozygote was used as the male parent carried the *cer7-3* mutant allele. These results support the inference that the double mutant is gametophytic lethal for both male and female gametophytes. Nevertheless, a few of the double mutant gametophytes must

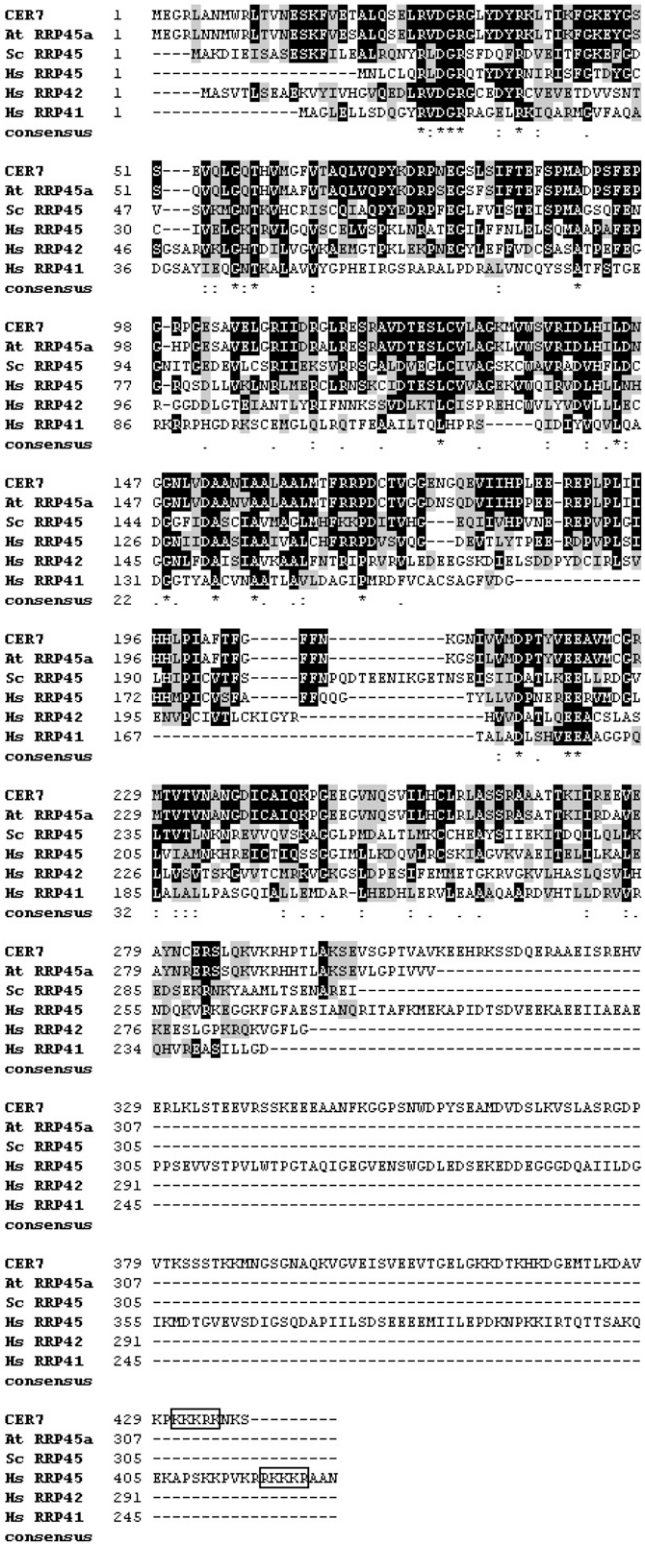

Figure 3. CER7 and At RRP45a Are Similar to Yeast RRP45 and Human PM/Scl-75.

Alignment of amino acid sequences of CER7 and At RRP45a with yeast RRP45 (Sc RRP45) and human RNase PH exosomal subunits PM/Scl-75 (Hs RRP45), RRP42, and RRP41 (Hs designation). Identical residues are indicated in black and similar residues in gray. The predicted nuclear localization signal is boxed.

survive. If the lethality were absolute, it would be impossible to obtain any F2 plants homozygous for one mutation and heterozygous for the other, unless the genetic background on the female parent affected the gametophytic viability. Rare transmission of the *cer7-3* allele in double mutant gametophytes, however, would explain the non-Mendelian segregation ratio obtained for the number of F2 progeny obtained from the *cer7-3*, At *rrp45a* cross that showed the *cer7* phenotype.

Regulation of Cuticular Wax Deposition by CER7

We examined transcript levels of *CER1*, *CER2*, *CER3/WAX2/YRE*, *CER4*, *CER5*, and *CER6* in the *cer7* mutant background to test if any of the wax-related genes that have been cloned might be regulated by CER7. Of these, only *CER3/WAX2/YRE* mRNA levels were significantly affected (data not shown). Reduced steady state levels of the *CER3/WAX2/YRE* mRNA in the *cer7* mutant (Figure 7A) suggested that CER7 acts as a positive regulator of *CER3/WAX2/YRE* transcription. To further dissect the *CER3/WAX2/YRE* transcriptional regulation by CER7, we monitored the expression of the bacterial β-glucuronidase (*GUS*) gene under the control of the *YRE* promoter (Kurata et al., 2003) in *cer7-1* and wild-type plants. As previously reported (Kurata et al., 2003), high levels of GUS activity were detected in wild-type stems and siliques expressing the Pro_{YRE}:GUS construct, whereas only residual GUS activity could be detected in the *cer7-1* mutant and exclusively in the abscission zone below the silique (Figures 7B and 7C). These results confirm that CER7 promotes the expression of *CER3/WAX2/YRE.* Since CER7 is a ribonuclease, it probably acts indirectly, possibly by degrading the transcript of a *CER3/WAX2/YRE* repressor. In the absence of functional CER7 protein in the *cer7* mutant, accumulation of such a repressor on the promoter of the *CER3/WAX2/YRE* gene would inhibit its transcription (Figure 8).

DISCUSSION

In a search for mutants deficient in regulation of cuticular wax biosynthesis, we identified the *cer7* line with decreased stem wax load due to a considerably reduced expression of the wax biosynthetic gene *CER3/WAX2/YRE.* We used the *cer7* mutant to clone the *CER7* gene and examined the role of CER7 in wax production.

The *cer7* mutation was found in *At3g60500*, one of the two *Arabidopsis* genes encoding proteins homologous to the yeast exosomal subunit RRP45p. Complementation of the *S. cerevisiae rrp45* mutant confirmed that CER7 is a functional homolog of yeast RRP45p, predicted to be one of the 3′-5′ exoribonucleases that form the core ring of the exosome, an evolutionarily conserved macromolecular complex involved in RNA processing and degradation (Raijmakers et al., 2004). The two *Arabidopsis* RRP45 proteins, designated At RRP45a and At RRP45b (CER7), have overlapping expression domains in *Arabidopsis* (Figures 5A and

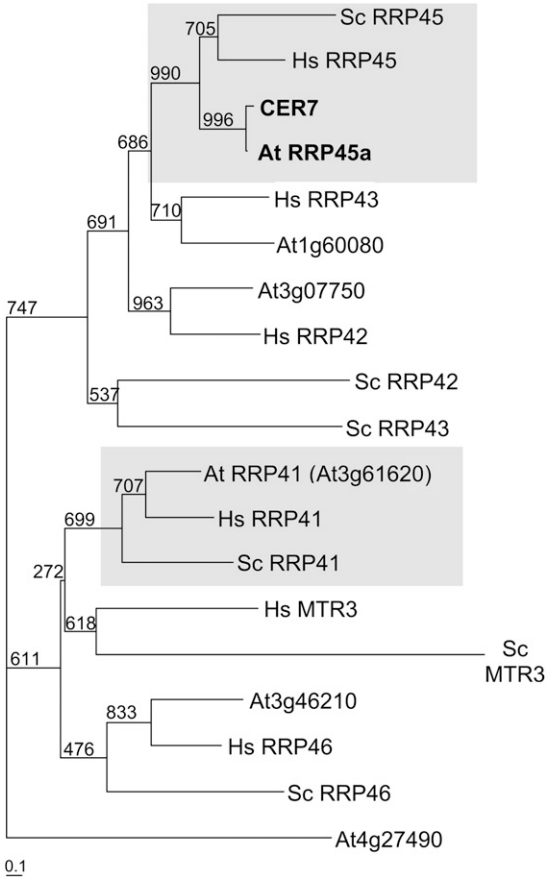

Figure 4. CER7 and At RRP45a Are Orthologs of Yeast RRP45 and Human PM/Scl-75.

Bootstrapped neighbor-joining phylogram of RNase PH-like exosomal proteins from *Arabidopsis* (At designations), yeast (Sc designations), and human (Hs designations). The clade including CER7 and the one including the well-characterized *Arabidopsis* homolog of Sc RRP41 are shaded.

5B), are distributed in the cytoplasm and the nucleus (Figure 5C), and when expressed under the control of the *CER7* promoter can both rescue wax deficiency of the *cer7* mutant (Figure 6B). However, while the *cer7* mutant exhibits a major reduction in cuticular wax load and low seed viability, the At *rrp45a* loss-of-function line does not show a pronounced wax phenotype or altered seed viability under the growth conditions used for this study. In addition, CER7 is superior to At RRP45a in complementing the yeast *rrp45* mutant and restoring growth of yeast cells (Figure 6A). Thus, it appears that these two proteins are not functionally identical and that CER7 is the major RRP45 homolog in *Arabidopsis*, whereas At RRP45a plays an accessory role.

Each of the 10 core exosomal components is essential for yeast viability (Houalla et al., 2006). Similarly, an analysis of the *Arabidopsis rrp4* null mutant demonstrated that the At RRP4 exosomal subunit is indispensable in a plant (Chekanova et al., 2002). The fact that *cer7* alleles are viable, but that the *cer7* At *rrp45a* double mutant is not, suggests that the At RRP45a homolog can perform the essential exosomal functions. In this respect, it is worth mentioning that At *RRP45a* is approximately twofold upregulated (data not shown) in the *cer7-3* mutant lacking CER7, which may be critical for its survival. Interestingly, however, the somewhat higher levels of At *RRP45a* expression did not alleviate wax deficiency of the *cer7-3* allele.

In yeast, partial loss-of-function mutations in different exosomal subunits sometimes result in very similar molecular phenotypes. This observation initially led to the proposal that an intact complex is required for exosome-mediated RNA processing and degradative functions (Mitchell et al., 1997; Anderson and Parker, 1998; Allmang et al., 1999b) but that individual subunits could also have some distinct functions. Recent work by several research groups revealed that there is indeed functional specialization of different core exosome subunits. For example, microarray analysis of global gene expression in several temperature-sensitive exosome mutants showed that distinct subpopulations of mRNA species accumulated in different mutant lines. Specifically, the absence of the nuclear exosome-associated subunit RRP6 in yeast caused an upregulation of mRNA species involved in cell wall biosynthesis and iron homeostasis (Houalla et al., 2006). It has also been reported that loss of RRP4 and RRP41 proteins resulted in unique developmental arrests, with the loss of RRP4 leading to aberrant embryogenesis and mutation in RRP41

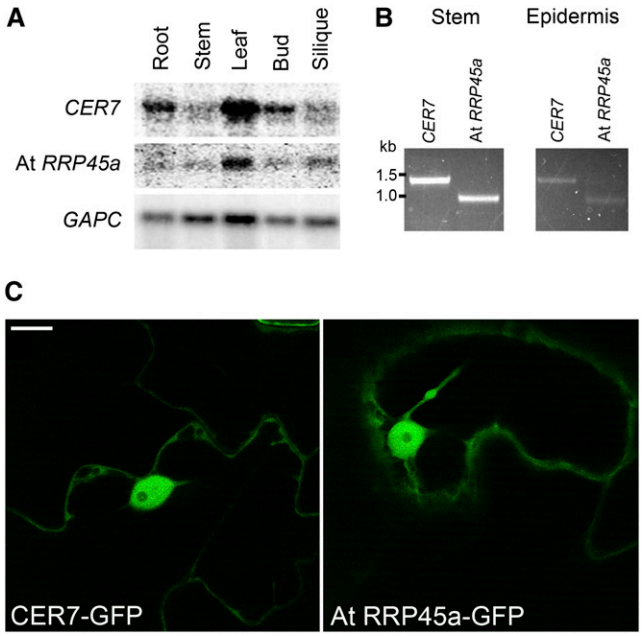

Figure 5. CER7 and At RRP45a Have Similar Expression Patterns and Subcellular Distributions.

(A) RNA gel blot analysis showing *CER7* and At *RRP45a* hybridization to total RNA isolated from roots, stems, leaves, flower buds, and siliques of *Arabidopsis*. *GAPC* was used as a loading control.

(B) RT-PCR amplification of *CER7* and At *RRP45a* using total RNA prepared from whole stems and from peeled stem epidermis.

(C) CER7-GFP and At RRP45a-GFP fusion proteins expressed in tobacco epidermal cells are localized in the cytoplasm and nucleoplasm of the nucleus but are excluded from the nucleolus. Bar = 10 μm.

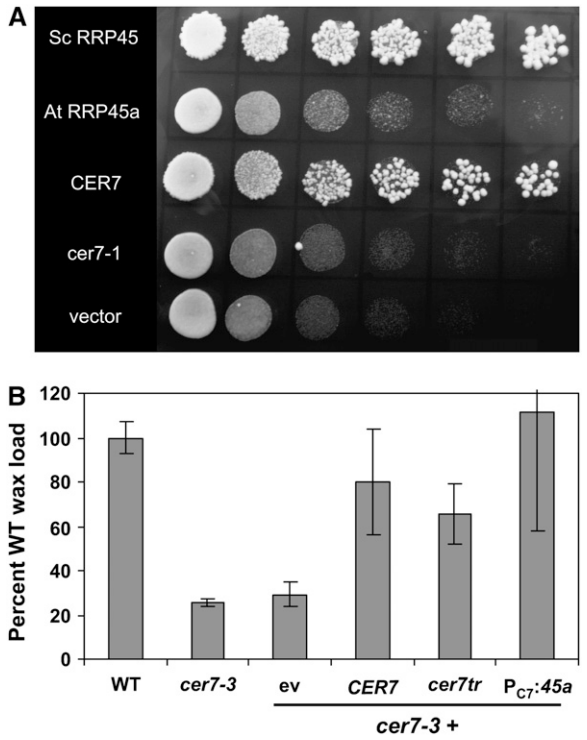

Figure 6. Functional Analysis of *CER7* and At *RRP45a*.

(A) The 10× serial dilutions of yeast strain YCA20 (*Δrrp45*) transformed with *GDP:*Sc *RRP45* (positive control), *GDP:*At *RRP45a*, *GDP:CER7*, *GDP:cer7-1*, or the empty vector.

(B) Stem cuticular wax loads relative to the wild type (Col-0) of *cer7-3* and *cer7-3* transformed with the empty vector (*cer7-3* + ev), *CER7* (*cer7-3* + *CER7*), *CER7* truncated to the length of At *RRP45a* (*cer7-3* + *cer7tr*), and At *RRP45a* driven by the *CER7* promoter (*cer7-3* + P_{C7}:*45a*). Bars represent means ± SD (n = 3, 3, 16, 14, 50, and 26).

affecting the female gametophyte (D.A. Belostotsky, personal communication). However, currently there are no other examples in eukaryotes of a core subunit of the exosome specifically influencing a cellular process, such as cuticular wax biosynthesis.

An alternative possibility that wax biosynthesis may not be sensitive to the loss of the CER7 subunit in particular but to a certain minimal level of functional exosome complex also needs to be considered in view of a recent report by Dziembowski et al. (2007). This study shows that the RRP44/Dis3 subunit alone is responsible for the yeast exosome core activity and suggests that the RNase PH subunits, including RRP45, are catalytically inactive members of the complex, serving as scaffolding and interacting with accessory proteins. If this is the case, *cer7* wax deficiency could be due to reduced activity of the exosome complex as a whole. However, another recent study of the structure and function of the exosome complex reported that the human RRP41/RRP45 dimer alone also has catalytic activity (Liu et al., 2007). Thus, at least this subcomplex may have a specialized role(s) in addition to its exosomal function.

The diverse cellular processes in which the exosome participates take place in the cytoplasm and the nucleus. The distribution of the exosome complex has been confirmed in these cellular locations, with the highest concentration reported in the nucleoli (Raijmakers et al., 2003, 2004). This is not the case with the CER7 protein in *Arabidopsis*. Our localization data show that CER7 is present in the cytoplasm and the nucleoplasm but excluded from the nucleolus (Figure 5C). Thus, CER7 may not be involved in nucleolar rRNA processing reactions. Furthermore, the absence of CER7 from the nucleolus suggests that various RNA processing and degradation functions of the exosome may not involve a complete set of core subunits. Instead, different subunits may act individually or by assembling into distinct subcomplexes as required for executing specialized functions, a model recently proposed for *Drosophila* (Graham et al., 2006).

Several lines of evidence support the idea that CER7 controls cuticular wax production in *Arabidopsis* stems by affecting the expression of CER3/WAX2/YRE, a key component of the decarbonylation pathway of wax biosynthesis in *Arabidopsis*. First,

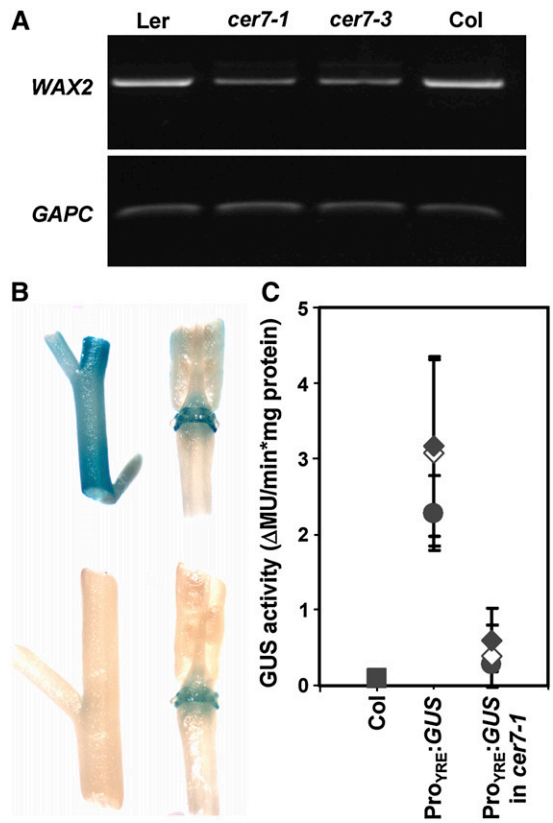

Figure 7. CER7 Regulates *CER3/WAX2/YRE* Transcription.

(A) RT-PCR analysis of *CER3/WAX2/YRE* and *GAPC* mRNA in *cer7-1* (*Ler*) and *cer7-3* (Col-0) stems and their corresponding wild types.

(B) Pro$_{YRE}$ -directed GUS expression in wild-type (top) and *cer7-1* (bottom) stem and silique segments.

(C) Quantitative assays of GUS activity in protein extracts of stems from three Pro$_{YRE}$:*GUS* transgenic lines in wild-type and *cer7-1* backgrounds. Each symbol represents the mean ± SD of three analyses of extracts obtained from three pooled individuals from each line; different symbols represent independent transformed lines. MU, 4-methylumbelliferone.

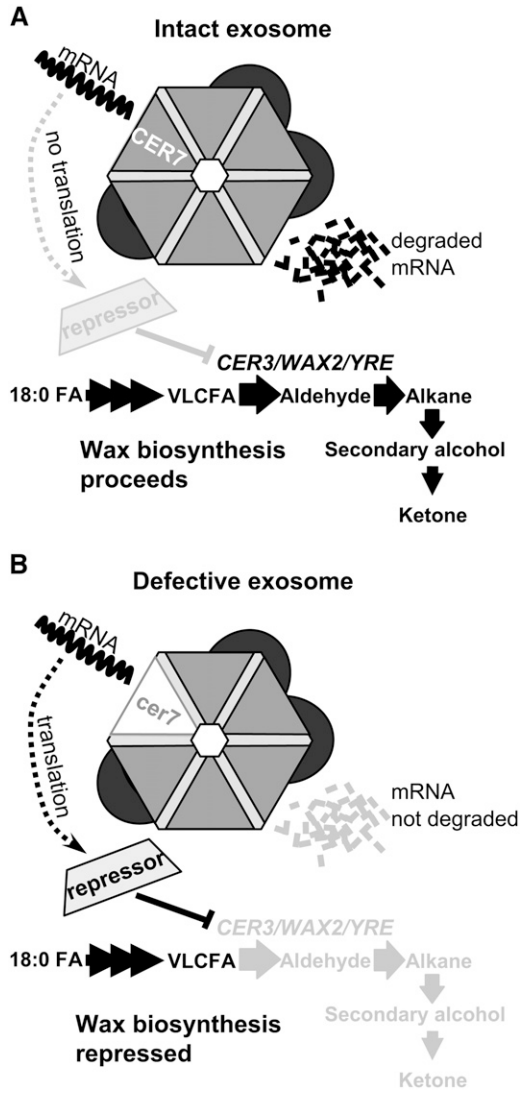

Figure 8. Model Illustrating CER7 Mode of Action.

(A) In the presence of CER7, mRNA encoding a hypothetical wax repressor is degraded, thus allowing the transcription of *CER3/WAX2/YRE* and wax production by the decarbonylation pathway.
(B) In the absence of CER7, the repressor protein inhibits *CER3/WAX2/YRE* transcription and wax production.

the stem wax composition of *cer7* mutants is very similar to that of *cer3* mutants (Goodwin et al., 2005), with substantial decreases in the compounds generated by the decarbonylation pathway and minimal effects on the primary alcohols, products of the acyl-reduction pathway. Second, the wax profile of the *cer3 cer7* double mutant is almost indistinguishable from that of either single mutant (data not shown), implicating the two genes in the same pathway. Third, *CER3/WAX2/YRE* transcript levels in the *cer7* mutant are reduced. Fourth, expression of the Pro_{YRE}:GUS reporter gene resulted in high levels of GUS activity in the wild type and virtually no GUS activity in the *cer7* mutant background, demonstrating that CER7 is required for transcription of the *CER3/WAX2/YRE* (Figure 7). However, since loss-of-function mutations in *CER7* result in reduced *CER3/WAX2/YRE* transcript accumulation, indicating that CER7 is a positive regulator of *CER3/WAX2/YRE* transcription and that CER7 probably causes degradation of its target, the CER7-mediated control of *CER3/WAX2/YRE* transcript levels is likely indirect. Our results support a model in which CER7 is required for degradation of a particular mRNA species specifying a repressor of *CER3/WAX2/YRE* transcription (Figure 8). In wild-type cells, CER7 ribonuclease would degrade the repressor, allowing wax production via the decarbonylation pathway to proceed. In *cer7* mutants, in the absence of CER7 activity, the repressor would not be degraded, and it would interfere with *CER3/WAX2/YRE* expression, consequently inhibiting wax production.

In summary, our results show that wax production in *Arabidopsis* is controlled, at least in part, by the mRNA stability of a repressor that is recognized and degraded by the CER7 ribonuclease. Identifying the mRNA target of the CER7 ribonuclease will be critical in defining the individual steps involved in this process.

METHODS

Plant Material and Growth Conditions

Arabidopsis thaliana mutant lines *cer7-1* (Koornneef et al., 1989), *cer7-2* (SALK_003100), and *cer7-3* (SAIL_747_B08) were obtained from the ABRC (www.arabidopsis.org), and At*rrp45a* (GABI_655D02) was ordered from GABI-Kat (Max Planck Institute for Plant Breeding Research). Plants were germinated on *Arabidopsis* agar plates (Somerville and Ogren, 1982) and grown in soil (Sunshine Mix 5; SunGro) at 20°C under continuous light (90 to 120 $\mu E/m^2/s$ PAR).

Cuticular wax was extracted and analyzed as reported by Millar et al. (1999).

Fine-Mapping and Cloning of CER7

To map the *cer7-1* mutation, *cer 7-1* (L*er*) was crossed with wild-type plants (Col-0), and genomic DNA from 605 F2 progeny with the *cer7* phenotype was extracted according to Dellaporta et al. (1983) or Klimyuk et al. (1993). Simple sequence length polymorphism or cleaved-amplified polymorphic sequence markers (Figure 2A) were used to pinpoint the *cer7-1* map position. Amplification conditions for ciw4, nga707, fus6.2, and nga6 (Bell and Ecker, 1994) and the tsh1-tsh9 markers designed based on polymorphisms listed in the Monsanto database (http://www.arabidopsis.org/Cereon/index.jsp; Jander et al., 2002) are available at The Arabidopsis Information Resource website (http://www.arabidopsis.org).

To complement the *cer7* mutant, a 3.8-kb genomic fragment containing the *At3g60500* coding sequence was amplified from wild-type (L*er*) genomic DNA using the primers 5′-TTAATGGTACCCTACATGATGTAG-TTTGTGTGTGC-3′ and 5′-TTAATGGGCCCTTCTCCTCTCCGATCTA-CCAGC-3′. PCR fragments were cloned into the pGREEN 0029 binary vector (Hellens et al., 2000) and transformed into *cer7-1* plants. Cuticular wax was extracted and analyzed from kanamycin-resistant T1 plants after visual screening for stem glaucousness.

The molecular lesion in *cer7-1* was identified by PCR amplification of the *CER7* genomic region from the wild type and *cer7-1* and sequencing. The sequences were compared using BioEdit 5.0.9 (Hall, 1999) to determine the location of the mutation.

To confirm the presence and positions of T-DNA insertions, genomic DNA isolated from individuals of each insertion line was used to amplify

gene-specific and insertion-specific fragments. The primers used were the Salk LBB1 primer, the SAIL LB3 primer, the GABI LB primer, and genomic DNA primers specific to each insertion site generated by the iSECT tool on the SIGnAL SALK website (http://signal.salk.edu/tdnaprimers.2.html) or GABI-Kat.

Construction of the Phylogenetic Tree

The amino acid sequences for the RNase PH exosomal subunits were aligned using the ClustalX program (Thompson et al., 1994, 1997) with default alignment parameters except for the protein matrix, for which BLOSUM62 (Henikoff and Henikoff, 1992) was used. The aligned sequences were imported into Bioedit for manual editing (Hall, 1999; http://www.mbio.ncsu.edu/BioEdit/bioedit.html). A number of unconserved regions were removed from the alignment (see Supplemental Figure 1 online) before construction of the phylogram. A bootstrapped neighbor-joining tree was generated using PHYLIP version 3.6 (distributed by the author, J. Felsenstein, 2005, University of Washington, Seattle) and visualized using TreeView (http://taxonomy.zoology.gla.ac.uk/rod/treeview.html).

RNA Gel Blot and RT-PCR Analysis

For RNA gel blot analysis, stem segments 2 cm long from just below the inflorescence, young leaves, unopened flower buds, young siliques, and roots from plants grown for 2 weeks in liquid *Arabidopsis* medium containing 3% sucrose were harvested and frozen in liquid nitrogen. Total RNA was extracted using TRIZOL reagent (Invitrogen Life Technologies) according to the manufacturer's protocol. Ten micrograms of total RNA from each sample was separated by electrophoresis on a 1% MOPS-agarose gel containing 5.8% formaldehyde. Separated RNA was downward-blotted (Koetsier et al., 1993) using 20× SSC as the transfer solution onto a Hybond XL membrane (Amersham) and fixed to the membrane by baking at 80°C for 2 h. Hybridization was performed in modified Church buffer (0.5 M Na-phosphate buffer, pH 7, 7% SDS, and 1 mM EDTA) overnight at 65°C using a PCR-generated ^{32}P-labeled DNA probe. Probe templates were amplified from cDNA, and probes were amplified from the purified templates using the primers 5′-TAGTGATAGCAGATAATGGAG-3′ and 5′-CTGCTTCTTACTTCCTCC-3′ for *CER7*; 5′-ATGGAGGGGAGGTTGAAT-3′ and 5′-ACAACTACAATAGGTCC-3′ for At *RRP45a*; and 5′-ACTCGAGAAAGCTGCTAC-3′ and 5′-ATTCGTTGTCGTACCATG-3′ for *GAPC* (cytosolic glyceraldehyde-3-phosphate dehydrogenase). Blots were washed in 2× SSC and 0.1% SDS (2 × 5 min); 1× SSC and 0.1% SDS (15 min); and 0.1× SSC and 0.1% SDS (2 × 10 min) at 65°C and then exposed to a phosphor screen that was scanned with a STORM 860 phosphor imager (Amersham Pharmacia Biotech).

For semiquantitative RT-PCR, total RNA was used for first-strand cDNA synthesis by SuperScript II polymerase (Invitrogen Life Technologies). For RT-PCR, cycle number and template amounts were optimized for all fragments amplified to yield products in the linear range of the reaction. Primer sequences and PCR conditions for each fragment were as follows: *CER7*, 5′-TAGTGATAGCAGATAATGGAG-3′ and 5′-CTGCTTCTTACTTCCTCC-3′, annealing temperature 50°C, number of cycles 27, extension time 60 s; At *RRP45a*, 5′-ATGGAGGGGAGGTTGAAT-3′ and 5′-ACAACTACAATAGGTCC-3′, annealing temperature 50°C, number of cycles 27, extension time 45 s; *WAX2*, 5′-GAGGCTCCTGTTGAGTTCCA-3′ and 5′-GCTTGCATCTCCTTTCACCT-3′, annealing temperature 55°C, number of cycles 28, extension time 50 s; *GAPC*, 5′-ACTCGAGAAAGCTGCTAC-3′ and 5′-ATTCGTTGTCGTACCATG-3′, annealing temperature 50°C, number of cycles 22, extension time 30 s.

GUS Assays

For the GUS histochemical assay, wild-type (Col-0) plants transformed with the Pro_{YRE}:GUS reporter gene obtained from Kurata et al. (2003) were crossed with *cer7-1* mutants, and F2 progeny were screened for a glossy-stem (*cer7-1*) phenotype. Plant tissues from the original transformed lines and from the *cer7-1* F2 progeny of the cross were incubated in GUS assay buffer (Jefferson, 1987) at 37°C for 0.5 h to overnight. The reaction was stopped by removal of the assay buffer and the addition of 95% ethanol. Samples were cleared by incubation in 95% ethanol overnight.

The GUS fluorometric assay was performed as described by Jefferson (1987). Briefly, 20 μL of crude protein extracts from the top 2 to 3 cm of stem material (excluding flowers and siliques) were added to GUS assay buffer containing 2 mM 4-methylumbelliferone-glucuronide. Protein concentrations were quantified against a BSA standard curve using the Bio-Rad protein assay, according to the manufacturer's protocol. The concentration of the hydrolysis product, 4-methylumbelliferone, in each reaction was measured by a plate-reading fluorometer (excitation at 365 + 7 nm; emission at 460 + 15 nm) at three successive time points. To determine the rates of 4-methylumbelliferone-glucuronide hydrolysis for different transgenic lines, the slopes of the curves were determined; these values were standardized to the protein concentrations of the extracts.

Plasmid Construction and Yeast and Plant Transformation

Yeast *RRP45* was amplified by yeast colony PCR using the primers 5′-TTAATGGATCCAATAGGAAACGGTTGCTAG-3′ and 5′-TATATCTCGAGGTCTTTCATACTGCCTTTAG-3′ and cloned into pBluescript II KS+/− (pBS; Stratagene) to yield pB/S:*RRP45. CER7* and *cer7-1* were amplified from *Arabidopsis* wild type (L*er*) and *cer7-1* cDNA, respectively, using the primers 5′-TTATTGAATTCTAGTGATAGCAGATAATGGAG-3′ and 5′-TTATAGAATTCAGAAAAGTACGAGTGATCGG-3′ and cloned into pENTR1A (Invitrogen) and pBS to yield pENTR1A:*CER7*, and pB/S:*cer7-1*. At *RRP45a* was amplified from wild-type cDNA using the primers 5′-TTATTGAATTCCTCACTAGCAAACAATGGAG-3′ and 5′-TATATTCTAGATACAATCGACGACCACAGC-3′ and cloned into pCR 2.1 (Invitrogen) to yield pCR:At *RRP45a*.

For expression in yeast, *RRP45*, *CER7*, *cer7-1*, and At *RRP45a* coding regions were subcloned into p426-GDP (Mumberg et al., 1995) and transformed into yeast (*Saccharomyces cerevisiae*) strain YCA20 (YDL 401 *Δrrp45* + *GAL10:RRP45*; Allmang et al., 1999a) by electroporation. Transformed cells were grown on restrictive YPAD (2% peptone, 1% yeast extract, 0.0075% adenine hemisulphate, and 2% glucose) medium for 4 d. Individual transformed colonies were cultured for 48 h in permissive YPARSG (2% peptone, 1% yeast extract, 0.0075% adenine hemisulphate, 2% raffinose, 2% sucrose, and 2% galactose) medium, and 5 μL each of six serial 10× dilutions were plated onto the YPAD medium. Equal starting cell titer for each line was confirmed by spotting 5 μL of the same dilutions onto YPARSG plates.

The *cer7tr* construct was made by site-directed mutagenesis using the reverse primer 5′-TAATAGGATCCCCTCCTACACAGCTACAGTAG-3′ with the forward primer 5′-TTATTGAATTCTAGTGATAGCAGATAATGGAG-3′ to introduce a stop codon into the *CER7* sequence at the point corresponding to the At *RRP45a* stop codon and to add an in-frame *Bam*HI restriction site. The cloned fragment containing the truncated version of *CER7* was cloned into pSL1180 (Pharmacia Biotech) to produce pSL1180:*cer7tr*, and the *CER7* genomic sequence (At3g60500) was subcloned from pGREEN 0029 into pMOG1006 (a gift from Mogen) to produce pMOG:*CER7. cer7tr* was then subcloned into pMOG:*CER7* using *Sph*I and *Bam*HI, replacing the wild-type *CER7* open reading frame to produce the vector pMOG:*cer7tr*. This construct was transformed into *cer7-3* plants. To make the Pro_{CER7}:At *RRP45a* construct, the 2-kb *CER7* 5′ promoter region was amplified using the primers 5′-TTATAGTCGACGCTTACAAATTACAAGGAGC-3′ and 5′-TTATTGGATCCTATCTGCTATCACTAGTAAAC-3′ and cloned into pBS. At *RRP45a* was subcloned from pCR:At *RRP45a* into pMOG1006, and then the *CER7* promoter was added.

Plant transformation was done by the floral dip method (Clough and Bent, 1998) or using a modification of this method in which plants sown at high density (100/4-inch pot) were sprayed, when the buds of their primary bolts were just visible, with a suspension of *Agrobacterium tumefaciens* strain GV3101 containing the transgene in a solution of 5% sucrose and 0.05% Silwet.

Subcellular Localization of GFP Fusion Proteins

CER7 and At *RRP45a* coding sequences were amplified from pENTR1A:*CER7* and pCR:At *RRP45a* to give PCR products that had in-frame fusion sites with the ATG (for N-terminal fusions) and with the stop codons deleted (for the C-terminal fusions). The fragments were cloned into pBluescript II SK+ (Stratagene), sequenced to confirm that there were no errors, and then subcloned into pVKH18-GFPN and pVKH18-GFPC (Zheng et al., 2005) to produce N- and C-terminal GFP fusion genes driven by the constitutive 35S promoter. The constructs were transiently expressed in tobacco (*Nicotiana tabacum*) epidermal cells by infusion via syringe as reported by Batoko et al. (2000), but with an infiltration buffer containing 50 mM MES, pH 5.6, 10 mM $MgCl_2$, and 150 μM acetosyringone (Sigma-Aldrich). GFP-derived fluorescence in the transformed cells was detected by confocal microscopy as reported by Zheng et al. (2005).

Accession Numbers

Sequence data from this article can be found in the GenBank/EMBL data libraries under the following accession numbers: *CER7* (*At3g60500*), DQ869270; At RRP45a (*At3g12990*), BT003077; and *CER3/WAX2/YRE* (*At5g57800*), AY131334 and AB099512.

Supplemental Data

The following material is available in the online version of this article.

Supplemental Figure 1. Amino Acid Alignment of RNase PH Exosome Subunits from *Saccharomyces cerevisiae* and *Homo sapiens*, and Similar Proteins from *Arabidopsis*, Used to Generate a Neighbor-Joining Phylogram (Figure 4)

ACKNOWLEDGMENTS

We thank George Haughn, Reinhard Jetter, and Xin Li for their insightful comments, the ABRC at Ohio State University for the SALK_003100 (*cer7-2*) and SAIL_747_B08 (*cer7-3*) lines, GABI-Kat for the GABI_655D02 (At *rrp45a*) line, T. Wada (Plant Science Center, RIKEN, Yokohama, Japan) for pYRE:GUS lines, and D. Tollervey (University of Edinburgh, UK) for the yeast *rrp45* mutant (YCA20) strain. The financial support of the Natural Sciences and Engineering Research Council of Canada is gratefully acknowledged.

Received November 30, 2006; revised February 1, 2007; accepted February 23, 2007; published March 9, 2007.

REFERENCES

Aharoni, A., Dixit, S., Jetter, R., Thoenes, E., van Arkel, G., and Pereira, A. (2004). The SHINE clade of AP2 domain transcription factors activates wax biosynthesis, alters cuticle properties, and confers drought tolerance when overexpressed in Arabidopsis. Plant Cell **16:** 2463–2480.

Allmang, C., Kufel, J., Chanfreau, G., Mitchell, P., Petfalski, E., and Tollervey, D. (1999b). Functions of the exosome in rRNA, snoRNA and snRNA synthesis. EMBO J. **18:** 5399–5410.

Allmang, C., Petfalski, E., Podtelejnikov, A., Man, M., Tollervey, D., and Mitchell, P. (1999a). The yeast exosome and human PM-Scl are related complexes of 3′-5′ exonucleases. Genes Dev. **13:** 2148–2158.

Alonso, J.M., et al. (2003). Genome-wide insertional mutagenesis of *Arabidopsis thaliana.* Science **301:** 653–657.

Anderson, J.S., and Parker, R.P. (1998). The 3′ to 5′ degradation of yeast mRNAs is a general mechanism for mRNA turnover that requires the SKI2 DEVH box protein and 3′ to 5′ exonucleases of the exosome complex. EMBO J. **17:** 1497–1506.

Batoko, H., Zheng, H.-Q., Hawes, C., and Moore, I. (2000). A Rab1 GTPase is required for transport between the endoplasmic reticulum and Golgi apparatus and for normal Golgi movement in plants. Plant Cell **12:** 2201–2218.

Bell, C.J., and Ecker, J.R. (1994). Assignment of 30 microsatellite loci to the linkage map of Arabidopsis. Genomics **19:** 137–144.

Broun, P., Poindexter, P., Osborne, E., Jiang, C.Z., and Riechmann, J.L. (2004). WIN1, a transcriptional activator of epidermal wax accumulation in Arabidopsis. Proc. Natl. Acad. Sci. USA **101:** 4706–4711.

Butler, J.S. (2002). The yin and yang of the exosome. Trends Cell Biol. **12:** 90–96.

Chekanova, J.A., Dutko, J.A., Mian, I.S., and Belostotsky, D.A. (2002). *Arabidopsis thaliana* exosome subunit AtRrp4p is a hydrolytic 3′→5′ exonuclease containing S1 and KH RNA-binding domains. Nucleic Acids Res. **30:** 695–700.

Chekanova, J.A., Shaw, R.J., Wills, M.A., and Belostotsky, D.A. (2000). Poly(A) tail-dependent exonuclease AtRrp41p from *Arabidopsis thaliana* rescues 5.8 S rRNA processing and mRNA decay defects of the yeast *ski6* mutant and is found in an exosome-sized complex in plant and yeast cells. J. Biol. Chem. **275:** 33158–33166.

Chen, X., Goodwin, S.M., Boroff, V.L., Liu, X., and Jenks, M.A. (2003). Cloning and characterization of the *WAX2* gene of Arabidopsis involved in cuticle membrane and wax production. Plant Cell **15:** 1170–1185.

Clough, S.J., and Bent, A.F. (1998). Floral dip: A simplified method for *Agrobacterium*-mediated transformation of *Arabidopsis thaliana.* Plant J. **16:** 735–743.

Dellaporta, S.L., Wood, J., and Hicks, J.B. (1983). A plant DNA minipreparation: Version II. Plant Mol. Biol. Rep. **1:** 19–21.

Dziembowski, A., Lorentzen, E., Conti, E., and Seraphin, B. (2007). A single subunit, Dis3, is essentially responsible for yeast exosome core activity. Nat. Struct. Mol. Biol. **14:** 15–22.

Goodwin, S.M., Rashotte, A.M., Rahman, M., Feldmann, K.A., and Jenks, M.A. (2005). Wax constituents on the inflorescence stems of double eceriferum mutants in Arabidopsis reveal complex gene interactions. Phytochemistry **66:** 771–780.

Graça, J., Schreiber, L., Rodrigues, J., and Pereira, H. (2002). Glycerol and glyceryl esters of omega-hydroxyacids in cutins. Phytochemistry **61:** 205–215.

Graham, A.C., Kiss, D.L., and Andrulis, E.D. (2006). Differential distribution of exosome subunits at the nuclear lamina and in cytoplasmic foci. Mol. Biol. Cell **17:** 1399–1409.

Hall, T.A. (1999). BioEdit: A user-friendly biological sequence alignment editor and analysis program for Windows 95/98/NT. Nucleic Acids Symp. Ser. **41:** 95–98.

Hellens, R.P., Edwards, E.A., Leyland, N.R., Bean, S., and Mullineaux, P.M. (2000). pGreen: A versatile and flexible binary Ti vector for *Agrobacterium*-mediated plant transformation. Plant Mol. Biol. **42:** 819–832.

Henikoff, S., and Henikoff, J.G. (1992). Amino-acid substitution matrices from protein blocks. Proc. Natl. Acad. Sci. USA **89:** 10915–10919.

Houalla, R., Devaux, F., Fatica, A., Kufel, J., Barrass, D., Torchet, C., and Tollervey, D. (2006). Microarray detection of novel nuclear RNA substrates for the exosome. Yeast **23:** 439–454.

Jander, G., Norris, S.R., Rounsley, S.D., Bush, D.F., Levin, I.M., and Last, R.L. (2002). Arabidopsis map-based cloning in the post-genome era. Plant Physiol. **129:** 440–450.

Jefferson, R.A. (1987). Assaying chimeric genes in plants: The GUS gene fusion system. Plant Mol. Biol. Rep. **5:** 387–405.

Klimyuk, V.I., Carroll, B.J., Thomas, C.M., and Jones, J.D. (1993). Alkali treatment for rapid preparation of plant material for reliable PCR analysis. Plant J. **3:** 493–494.

Koetsier, P.A., Schorr, J., and Doerfler, W. (1993). A rapid protocol for downward alkaline Southern blotting of DNA. Biotechniques **15:** 260–262.

Koornneef, M., Hanhart, C.J., and Thiel, F. (1989). A genetic and phenotypic description of *eceriferum* (*cer*) mutants in *Arabidopsis thaliana.* J. Hered. **80:** 118–122.

Kunst, L., Jetter, R., and Samuels, A.L. (2006). Biosynthesis and transport of plant cuticular waxes. In Biology of the Plant Cuticle, M. Riederer and C. Müller, eds (Oxford, UK: Blackwell Publishing), pp. 182–215.

Kunst, L., and Samuels, A.L. (2003). Biosynthesis and secretion of plant cuticular wax. Prog. Lipid Res. **42:** 51–80.

Kurata, T., Kawabata-Awai, C., Sakuradani, E., Shimizu, S., Okada, K., and Wada, T. (2003). The *YORE-YORE* gene regulates multiple aspects of epidermal cell differentiation in Arabidopsis. Plant J. **36:** 55–66.

Li, Y., Rosso, M.G., Strizhov, N., Viehoever, P., and Weisshaar, B. (2003). GABI-Kat SimpleSearch: A flanking sequence tag (FST) database for the identification of T-DNA insertion mutants in *Arabidopsis thaliana.* Bioinformatics **19:** 1441–1442.

Liu, Q., Greimann, J.C., and Lima, C.D. (2007). Reconstitution, activities and structure of the eukaryotic RNA exosome. Cell **127:** 1223–1237.

Lolle, S.J., Hsu, W., and Pruitt, R.E. (1998). Genetic analysis of organ fusion in *Arabidopsis thaliana.* Genetics **149:** 607–619.

Millar, A.A., Clemens, S., Zachgo, S., Giblin, E.M., Taylor, D.C., and Kunst, L. (1999). *CUT1*, an Arabidopsis gene required for cuticular wax biosynthesis and pollen fertility, encodes a very-long-chain fatty acid condensing enzyme. Plant Cell **11:** 825–838.

Mitchell, P., Petfalski, E., Shevchenko, A., Mann, M., and Tollervey, D. (1997). The exosome: A conserved eukaryotic RNA processing complex containing multiple 3′→5′ exoribonucleases. Cell **91:** 457–466.

Mumberg, D., Muller, R., and Funk, M. (1995). Yeast vectors for the controlled expression of heterologous proteins in different genetic backgrounds. Gene **156:** 119–122.

Nawrath, C. (April 4, 2002). The biopolymers cutin and suberin. In The Arabidopsis Book, C.R. Somerville and E.M. Meyerowitz, eds. (Rockville, MD: American Society of Plant Biologists), doi/10.1199/tab.0021, http://www.aspb.org/publications/arabidopsis/.

Pighin, J.A., Zheng, H., Balakshin, L.J., Goodman, I.P., Western, T.L., Jetter, R., Kunst, L., and Samuels, A.L. (2004). Plant cuticular lipid export requires an ABC transporter. Science **306:** 702–704.

Raijmakers, R., Egberts, W.V., van Venrooij, W.J., and Pruijn, G.J.M. (2003). The association of the human PM/Scl-75 autoantigen with the exosome is dependent on a newly identified N terminus. J. Biol. Chem. **278:** 30698–30704.

Raijmakers, R., Schilders, G., and Pruijn, G.J. (2004). The exosome, a molecular machine for controlled RNA degradation in both nucleus and cytoplasm. Eur. J. Cell Biol. **83:** 175–183.

Rosso, M.G., Li, Y., Strizhov, N., Reiss, B., Dekker, K., and Weisshaar, B. (2003). An *Arabidopsis thaliana* T-DNA mutagenized population (GABI-Kat) for flanking sequence tag-based reverse genetics. Plant Mol. Biol. **53:** 247–259.

Sessions, A., et al. (2002). A high-throughput Arabidopsis reverse genetics system. Plant Cell **14:** 2985–2994.

Sieber, P., Schorderet, M., Ryser, U., Buchala, A., Kolattukudy, P., Metraux, J.P., and Nawrath, C. (2000). Transgenic Arabidopsis plants expressing a fungal cutinase show alterations in the structure and properties of the cuticle and postgenital organ fusions. Plant Cell **12:** 721–738.

Somerville, C.R., and Ogren, W.L. (1982). Isolation of photorespiratory mutants of Arabidopsis. In Methods in Chloroplast Molecular Biology, R.B. Hallick and N.H. Chua, eds (New York: Elsevier), pp. 129–139.

Thompson, J.D., Gibson, T.J., Plewniak, F., Jeanmougin, F., and Higgins, D.G. (1997). The CLUSTAL X windows interface: Flexible strategies for multiple sequence alignment aided by quality analysis tools. Nucleic Acids Res. **25:** 4876–4882.

Thompson, J.D., Higgins, D.G., and Gibson, T.J. (1994). CLUSTAL W: Improving the sensitivity of progressive multiple sequence alignment through sequence weighting, position-specific gap penalties and weight matrix choice. Nucleic Acids Res. **22:** 4673–4680.

Zhang, J.Y., Broeckling, C.D., Blancaflor, E.B., Sledge, M.K., Sumner, L.W., and Wang, Z.Y. (2005). Overexpression of WXP1, a putative *Medicago truncatula AP2* domain-containing transcription factor gene, increases cuticular wax accumulation and enhances drought tolerance in transgenic alfalfa (*Medicago sativa*). Plant J. **42:** 689–707.

Zheng, H., Rowland, O., and Kunst, L. (2005). Disruptions of the Arabidopsis enoyl-CoA reductase gene reveal an essential role for very-long-chain fatty acid synthesis in cell expansion during plant morphogenesis. Plant Cell **17:** 1467–1481.